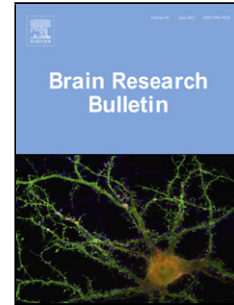


## Accepted Manuscript

Title: MESENCHYMAL STEM CELL THERAPY  
IMPROVES SPATIAL MEMORY AND HIPPOCAMPAL  
STRUCTURE IN AGING RATS

Authors: Maria F. Zappa Villar, Marianne Lehmann, Mariana  
G. García, Guillermo Mazzolini, Gustavo R. Morel, Gloria M.  
Cónsole, Osvaldo Podhajcer, Paula C. Reggiani, Rodolfo G.  
Goya



PII: S0166-4328(18)31533-X  
DOI: <https://doi.org/10.1016/j.bbr.2019.04.001>  
Reference: BBR 11887

To appear in: *Behavioural Brain Research*

Received date: 10 November 2018  
Revised date: 31 March 2019  
Accepted date: 1 April 2019

Please cite this article as: Zappa Villar MF, Lehmann M, García MG, Mazzolini G, Morel GR, Cónsole GM, Podhajcer O, Reggiani PC, Goya RG, MESENCHYMAL STEM CELL THERAPY IMPROVES SPATIAL MEMORY AND HIPPOCAMPAL STRUCTURE IN AGING RATS, *Behavioural Brain Research* (2019), <https://doi.org/10.1016/j.bbr.2019.04.001>

This is a PDF file of an unedited manuscript that has been accepted for publication. As a service to our customers we are providing this early version of the manuscript. The manuscript will undergo copyediting, typesetting, and review of the resulting proof before it is published in its final form. Please note that during the production process errors may be discovered which could affect the content, and all legal disclaimers that apply to the journal pertain.

Ref: BBR-2018-1394-R2 (Clean)

## MESENCHYMAL STEM CELL THERAPY IMPROVES SPATIAL MEMORY AND HIPPOCAMPAL STRUCTURE IN AGING RATS

Maria F. **Zappa Villar**<sup>ab1</sup>, Marianne **Lehmann**<sup>ab1</sup>, Mariana G. **García**<sup>c</sup>, Guillermo **Mazzolini**<sup>c</sup>, Gustavo R. **Morel**<sup>ab</sup>, Gloria M. **Cónsole**<sup>b</sup>, Osvaldo **Podhajcer**<sup>d</sup>, Paula C. **Reggiani**<sup>ab2</sup>, Rodolfo G. **Goya**<sup>ab2</sup>

<sup>a</sup>INIBIOLP-Pathology B, School of Medicine, National University of La Plata.

<sup>b</sup>Department of Histology and of Embryology B, School of Medicine, National University of La Plata, Argentina.

<sup>c</sup>Gene Therapy Laboratory, IIMT, School of Medical Science, Austral University, Buenos Aires, Argentina.

<sup>d</sup>Laboratory of Molecular and Cellular Therapy, Fundacion Instituto Leloir, Buenos Aires, Argentina.

\***Corresponding author:** Rodolfo G. Goya INIBIOLP

School of Medicine, UNLP, 60 and 120 streets 1900 - La Plata, Argentina [goya@isis.unlp.edu.ar](mailto:goya@isis.unlp.edu.ar) Tel. 54-221-4256735

Please, CC [paulareggiani@conicet.gov.ar](mailto:paulareggiani@conicet.gov.ar)

**Running title:** Stem cell therapy and memory in old rats

<sup>1</sup> These two authors contributed equally to this study.

<sup>2</sup> These two senior authors contributed equally to this study.

## HIGHLIGHTS

- Mesenchymal stem cells (MSCs) are of interest for the treatment of brain pathologies
- Spatial memory in aged female rats significantly improved after MSC administration
- Hippocampal neurogenesis increased after MSC treatment in aging rats
- MSCs have an important role in microglia and synaptic protein remodeling

## ABSTRACT

There is a growing interest in the potential of mesenchymal stem cells (MSCs) for implementing regenerative medicine in the brain as they have shown neurogenic and immunomodulatory activities. We assessed the effect of intracerebroventricular (icv) administration of human bone marrow-derived MSCs (hBM-MSCs) on spatial memory and hippocampal morphology of senile (27 months) female rats, using 3-months-old counterparts as young controls. Half of the animals were injected in the lateral ventricles (LV) with a suspension containing  $5 \times 10^5$  hBM-MSCs in 8  $\mu$ l per side. The other half received no treatment (senile controls). Spatial memory performance was assessed with a modified version of the Barnes maze test. We employed one probe trial, one day after training in order to evaluate learning ability as well as spatial memory retention. Neuroblast (DCX) and microglial (Iba-1 immunoreactive) markers were also immunohistochemically quantitated in the animals by means of an unbiased stereological approach. In addition, hippocampal presynaptic protein expression was assessed by immunoblotting analysis. After treatment, the senile MSC-treated group showed a significant improvement in spatial memory accuracy and extended permanence in a one- and 3-hole goal sectors as compared with senile controls. The MSC treatment increased the number of neuroblasts in the hippocampal dentate gyrus, reduced the number of reactive microglial cells, and restored presynaptic protein levels as compared to senile controls. We conclude that icv injected hBM-MSCs are effective in improving spatial memory in senile rats and that the strategy improves some functional and morphologic brain features typically altered in aging rats.

**Keywords.** Brain aging- memory- hippocampus- mesenchymal stem cells – cell therapy

## 1.-INTRODUCTION

There is a growing interest in the therapeutic potential of adult mesenchymal stem cells (MSCs) in the brain. One type of adult stem cell that has been used for this purpose are the bone marrow-

derived MSCs. They are known to secrete neurotrophic factors and promote the survival, proliferation and differentiation of neural cells *in vitro* [1, 2]. See Discussion for further details on the neuroactive factors released by MSC.

MSCs are easily isolated and expanded from bone marrow and even from adipose tissues, amniotic fluid, endometrium, dental tissues, umbilical cord. They are multipotent adult stem cells with the capacity to differentiate into mesodermal lineage such as osteocytes, adipocytes and chondrocytes[3]. However, MSCs also show differentiation plasticity into other endodermal lineages (hepatocytes) and ectodermal (neurocytes), including neurons and glial cells [4]. In addition to their neural differentiation ability under special conditions, MSCs are known for their capacity to promote neurogenesis of primary neural progenitors and survival of neural cells, by expressing neurotrophic factors, such as brain-derived neurotrophic factor (BDNF), nerve growth factor (NGF), and insulin-like growth factor-1 [5, 6]. The level of these neurotrophic factors is severely affected in aging and can be correlated with cognitive decline [7, 8].

Transplantation of MSCs in the central nervous system prevents apoptosis and promotes neurogenesis (proliferation and differentiation) of ‘host’ neural cells and stem cells in the engrafted site [5, 9, 10]. MSCs were therefore suggested as candidates for treating a variety of neurodegenerative diseases, in particular Parkinson’s disease (PD), multiple sclerosis, cerebral hemorrhage and brain cancer [11–13]. Intracerebroventricular (icv) injection of bone marrow-derived MSCs increased hippocampal neurogenesis in a rat model of depression. Thus, after transplantation, MSCs migrated mainly to the dentate gyrus (DG), CA1 and CA3 regions of the hippocampus, and to a lesser extent to the thalamus, hypothalamus, cortex and contralateral hippocampus. Neurogenesis was increased in the ipsilateral DG of engrafted rats (granular cell layer). The level of engraftment was positively correlated with behavioral performance [14]. Sites such as the hippocampus, subventricular zone and optic bulb, where active neurogenesis occurs in adulthood, are often preferred for engraftment of MSCs [15, 16].

In females *Sprague-Dawley* (SD) rats, spatial memory impairment begins at 14 months, with greater impairment at 20 to 26 months [17]. Furthermore, immune reactivity and inflammatory processes increase with aging in the brain [18], with microglia playing a central role in this immune dysregulation [19, 20]. We have recently shown that in aging female rats there is a significant activation of reactive microglia and identified a cluster of hippocampal immune genes that are dysregulated in the aged animals [21]. Interestingly, it was reported that MSCs are able to maintain the resting phenotype of microglia and can also control its activation through the release of several factors, including but not limited to, vascular endothelial growth factor (VEGF), brain-derived neurotrophic factor (BDNF), glial-derived neurotrophic factor (GDNF) and hepatocyte growth factor (HGF), which suggests that MSCs could be a promising therapeutic tool for treatment of diseases associated with microglial activation [22]. The above information prompted us to explore the neuroprotective potential of human bone marrow-derived MSCs (hBM-MSCs) in the hippocampus of senile rats at both functional and morphological level.

## **2.- MATERIALS AND METHODS**

### **2.1- Human bone marrow-derived mesenchymal stem cells**

Human BM-MSCs were isolated from bone marrow aspirates of healthy donors for allogeneic transplantation after informed consent approved by the Institutional Review Committee of Hospital Naval Pedro Mallo and Fundación Instituto Leloir, Argentina and according to the International Society for Cellular Therapy (ISCT) guidelines. Human MSCs were characterized as described previously [23], cultured in complete DMEM low glucose (2  $\mu$ M glutamine, 100 U/ml penicillin, 100 mg/ml streptomycin) and 20% heat-inactivated fetal bovine serum (FBS), and used between passages 4 to 7.

### **2.2- Fluorescent labeling of MSCs**

Human BM-MSCs cultures were grown in Petri dishes to 90% confluence. Suspended MSCs were labeled with 1,10-dioctadecyl-3,3,30,30-tetramethylindocarbocyanine perchlorate (Dil, Sigma Chem Co.) fluorescent dye (stock solution: 0.25 µg of Dil per microliter of dimethylsulfoxide). Briefly, trypsinized MSCs were suspended in phosphate buffered saline (PBS, 10<sup>6</sup> cells/ml) in the presence of Dil at a final concentration of 1 µg/ml and incubated for 5 min at 37°C followed by 15 min at 4°C and finally washed 3 times with PBS. An appropriate dilution (6.25 X 10<sup>4</sup> MSCs/µl) for the icv injection was made.

### 2.3- Animals and experimental design

Young (3 mo.) and senescent (27 mo.) female SD rats were used. The animals were housed in a temperature-controlled room (22 ± 2°C) on a 12:12 h light/dark cycle. Food and water were available *ad libitum*. All experiments with animals were performed in accordance to the Animal Welfare Guidelines of NIH (INIBIOLP's Animal Welfare Assurance No A5647-01).

Rats were grouped, as follows: **Group Yc**, consisted of 8 young rats that received no treatment. **Group Sc**, consisted of 8 senescent rats that received no treatment and **Group Smsc**, consisted of 8 senescent rats that were stereotaxically injected with MSCs.

The day of MSCs injection was defined as experimental day **0**. Before and after cell injection, a full Barnes maze test, comprising 6 acquisition trials (AT) and a probe trial was performed on all rats. Additional young rats were used for time-course studies.

**Experimental design**- Nine days before the MSCs injection (experimental day -9) the pre-treatment Barnes maze test began. On experimental day 0, old rats were icv injected with MSCs as described below. From experimental day 15 to 18, all rats were submitted to the post-treatment Barnes maze test (**Fig 1 A**). On experimental day 21, all rats were euthanized as described below.

**2.4- Time-course design**- Additional young rats (N=8) were used for time-course studies. On

experimental day 0, rats were icv injected with Dil-labeled MSCs as described below. At different time-points, on experimental day 5, 11, 14 and 21, two rats were sacrificed as described below. Brains were processed as previously described for immunohistochemical assessment to analyze the distribution and permanence of injected cells (**Fig 1 B**).

## 2.5- Stereotaxic injections

Rats were anesthetized with ketamine hydrochloride (40 mg/kg; ip) plus xylazine (8 mg/kg; im) and placed in a stereotaxic apparatus. In order to access the LV, the tip of a 26G needle fitted to a 10  $\mu$ l syringe was brought to the following coordinates relative to the bregma: -0.8 mm anteroposterior, 4.1 mm dorsoventral and  $\pm$ 1.5 mm mediolateral [24]. The animals were injected bilaterally with 8  $\mu$ l per side of a suspension containing  $5 \times 10^5$  MSCs.

## 2.6- Spatial memory assessment

A modified Barnes maze protocol was used in this study; it is based on a previously reported procedure [25]. It consists of an elevated (108 cm to the floor) black acrylic circular platform, 122 cm in diameter, containing twenty holes around the periphery. The holes are of uniform diameter (10 cm) and appearance, but only one hole is connected to a black escape box (tunnel). The escape box is 38.7 cm long x 12.1 cm wide x 14.2 cm in depth and it is removable. A white cylindrical starting chamber (an opaque, 20 cm x 30 cm long, and 15 cm high, open-ended chamber) is used to place the rats on the platform. Four proximal visual cues are placed in the room, 50 cm away from the circular platform. The escape hole was numbered as hole 0 for graphical normalized representation purposes, the remaining holes being numbered 1 to 10 clockwise, and -1 to -9 counterclockwise (**Fig 3A**). Hole 0 remained in a fixed position, relative to the cues in order to avoid randomization of the relative position of the escape box. During the test, the platform was rotated daily. A90-dB white-noise generator and a white-light 500 W bulb provided the escape stimuli from the platform.

We used an shortened protocol based on three days of acquisition trials (AT), followed by a probe trial, 1 day after training, to assess recent spatial memory retention [26]. An acquisition trial consists of placing a rat, randomly oriented, in the starting chamber for 30 s, the chamber is then raised, the aversive stimuli are switched on and the rat is allowed to freely explore the maze for 120 s. Probe trial is defined as a trial where the escape box has been removed, its purpose being to assess the latency to explore the empty escape hole and the error frequency. After the starting chamber is raised, the rat is given 120 s to explore and the number of explorations per hole is recorded. In order to eliminate olfactive clues from the maze and the boxes, the surfaces are cleaned with 10% ethylic alcohol solution, after each trial. On the day before acquisition trial, animals were habituated to the starting chamber and escape box by placing them inside each one for 180s.

The behavioral performances were recorded using a computer-linked video camera mounted 110 cm above the platform. The video-recorded performances of the subjects were measured using the Kinovea v0.7.6 (<http://www.kinovea.org>) software. The behavioral parameters assessed were as follows.

**Escape box latency:** time (in s) spent by an animal since its release from the starting chamber until it enters the escape box (during an acquisition trial) or until the first exploration of the escape hole (during a probe trial).

**Goal sector exploration frequency (GS):** the sum of the number of explorations for holes -1, 0, and 1 divided by 3 (**GS3**) or the number of explorations of hole 0 (**GS1**), during a probe trial.

**GS3 progression index:** this parameter results from the difference between the frequency of final (post-treatment) minus the initial exploration(pre-treatment).

## 2.7- Sample preparation

Animals were placed under deep anesthesia and transcardially perfused with phosphate buffered para- formaldehyde 4%, (pH 7.4) fixative. The brains were rapidly removed and stored in para-

formaldehyde 4%, (pH 7.4) overnight (4 °C). Finally, brains were maintained in cryopreservative solution (30% ethylene glycol, 1% polyvinylpyrrolidone, 30% sucrose, in phosphate buffer 0.1 M, pH 7.4) at -20 °C until use. For immunohistochemical assessment, brains were cut coronally in 40 µm-thick sections with a vibratome (VT1000S; Leica Microsystems, Wetzlar, Germany). The rest of the animals were quickly decapitated, and the hippocampus carefully dissected as previously described [27] and stored at -80 °C until WB analysis.

## 2.8- Immunohistochemistry

All immunohistochemical techniques were performed on free-floating sections. For each animal, separate sets of sections were immunohistochemically processed using anti-doublecortin (DCX) goat polyclonal antibody 1:250 (c-18, Santa Cruz Biotech., Dallas, Texas) and anti-Iba-1 rabbit polyclonal antibody 1: 1000 (016-20001, Wako Chemicals, Richmond, VA, USA). For detection, the Vectastain® Universal ABC kit (1:500, PK-6100, Vector Labs., Inc., Burlingame, CA, USA) employing 3, 3-diamino benzidine tetrahydro-chloride (DAB) as chromogen, was used. Briefly, after overnight incubation at 4°C with the primary antibody, sections were incubated with biotinylated horse anti-mouse antiserum (1:300, BA- 2000, Vector Labs.) or horse anti-goat antiserum (1:300, BA-9500, Vector Labs), as appropriate, for 120 min, rinsed and incubated with avidin-biotin-peroxidase complex (ABC Kit) for 90 min and then incubated with DAB. Sections were counterstain with Nissl method (0.5% cresyl violet solution at 37°C for 10 min) to visualize anatomical landmarks and mounted with Vectamount (Vector Labs) to use for image analysis.

## 2.9- Image Analysis

In each hippocampal block, every sixth serial sections were selected in order to obtain a set of non-contiguous serial sections spanning the dorsal hippocampus (240 µm apart). The number of cells was

assessed in the dorsal hippocampus which is located between coordinates -2.8 mm to -4.5 mm from the bregma [24] using an Olympus BX-51 microscope, at 500X magnification, attached to an Olympus DP70 CCD video camera (Tokyo, Japan). The total number of cells was estimated using a modified version of the optical dissector method [28]. Individual estimates of the total bilateral cell number (N) were calculated according to the following formula:  $N = RQ\Sigma \cdot 1/ssf \cdot 1/asf \cdot 1/tsf$ , where  $RQ\Sigma$  is the sum of counted cells,  $ssf$  is the section sampling fraction,  $asf$  is the area sampling fraction, and  $tsf$  is the thickness sampling fraction.

### 2.10- Neuroblast analysis

The number of DCX positive neuroblasts was assessed using a modified version of the optical fractionator technique [28]. The entire subgranular zone (SGZ) and granular cell layer (GCL) regions were quantified (8 sections per animal), with  $asf=1$ ,  $ssf=1/6$  and  $tsf=1$ . Estimates were based on counting DCX(+) cell bodies as they came into focus. N= 4 animals per group.

### 2.11- Microglial cell analysis

Microglial cells were identified as Iba-1 immunoreactive cells. Iba-1 immunoreactive cells were counted in the Srad of the CA1 region of the dorsal hippocampus. The Srad upper limit is the *pyramidal layer*, lower limit is *Stratum Lacunosum Moleculare* and the lateral limit is the *Stratum Lucidum* [24]. To this end, a random grid consisting of squared probes (area=22,500  $\mu\text{m}^2$ ) was superimposed over calibrated images taken at 600X magnification (3 fields per section, 6-8 sections per animal) and cells inside the probe area were counted. Cells making contact with boundary inclusion lines of the probes were included in the count, whereas cells in contact with boundary exclusion lines were not counted. Iba-1 immunoreactive cells were morphologically classified as type I, II, III, IV and V on the basis of previously documented criteria [26, 29]. Type I, cells with few cellular processes (two or less); Type II, cells showing three to five short branches; Type III, cells

with numerous (>5) and longer cell processes and a small cell body; Type IV, cells with large somas and retracted and thicker processes and Type V, cells with amoeboid cell body, numerous short processes and intense Iba-1 immunostaining. Types I, II and III were categorized as nonreactive glia whereas types IV and V were taken as reactive glia. Reactive microglial cell number/section was calculated for each animal with  $asf=0.387$ ,  $ssf=1/6$ , and  $tsf=1$ . N= 4 animals per group.

## 2.12 Western Blot Analysis

### 2.12.1 Sample preparation

In order to obtain protein lysates, hippocampi were homogenized with precooled RIPA buffer (150 mM NaCl, 1% Triton X-100, 0.5 % sodium deoxycolate, 0.1 % SDS, 50 mM Tris-HCl pH 8, and appropriate protease inhibitors, pH 7.4). Finally, protein concentration was measured by Bradford protein assay. Bovine serum albumin (BSA) (0.1-1 mg/ml) was used as a standard. Samples were aliquoted and stored at  $-80^{\circ}\text{C}$ .

### 2.12.2 Immunoblotting

Equal amounts of protein (50  $\mu\text{g}$ ) for every sample were separated by 10% SDS-PAGE and transferred to nitrocellulose membranes (Bio-Rad). The membranes were blocked by incubation in 5% non-fat milk in Tris-buffered saline/Tween-20 (TBS-T) for 1 h at room temperature, and then incubated with primary antibodies against Synaptotagmin 1 (SYT1, 1:200; mAb 48, DSHB), Synaptophysin (SYP, 1:200; sc-17750, Santa Cruz Biotech.), Postsynaptic density protein 95 (PSD-95, 1:200, sc-32290, Santa Cruz Biotech.), Vinculin (VIN) (1:200; sc-73614, Santa Cruz Biotech.) and  $\beta$ -Actin (1:1000, sc-47778, Santa Cruz Biotech.) overnight at  $4^{\circ}\text{C}$ . Then, the membranes were washed with TBS-T and incubated with anti-mouse secondary antibody conjugated with horseradish peroxidase (1:10000, #115-035-003, Jackson ImmunoResearch Laboratories) for 3 h at room temperature. After washing with TBS-T, membrane visualization was performed with Super Signal

West Pico PLUS Chemiluminescent substrate (#34577, Thermo Fisher Scientific) on a Chemidoc Image Station (Bio-Rad, Hercules, CA, USA). Relative optical density of protein bands was analyzed using gel documentation system. Sample loading was normalized to relative density of VIN or  $\beta$ -Actin band. Four rats per group were used for the WB .

### 2.13 -Statistical analysis

Data were compiled and analyzed with the Sigma Plot v. 11 software (San Jose, CA). The analysis of repeated measurements (rm) of ANOVA was applied over the data obtained from behavioral tests. Wilcoxon matched-pairs signed rank test was employed for GS3 analysis. For determine MSCs rejuvenated effect ANOVA was used (Iba-1 immunohistochemistry and SYT1 immunoblotting). Otherwise, stereological assessment of senile groups data was examined by Unpaired Student t-test. All data are represented as mean  $\pm$  SEM. Holm-Sidak and Tukey's post-hoc tests were used where appropriate. Criteria for significant differences were set at 95% probability level.

## 3.-RESULTS

### 3.1- Time-course of MSC in the cerebral ventricles

Dil-fluorescence in coronal sections of MSCs-injected young brains revealed that five days after injection, Dil-labeled hBM-MSCs were located in close contact with the ependymal cells. The number of labeled cells decreased progressively from experimental day 5. On the day of sacrifice (21) labeled cells were still observable close to the ependymal layers (**Fig 1B**). However, some of these cells traveled a short distance from the ventricular spaces to the parenchyma (**Fig 1B**).

### 3.2- Cognitive Changes

**3.2.1- Hole exploration frequency-** As expected, hole exploration frequency showed a bell-shaped distribution around hole 0 in the probe trial in all three groups both before and after treatment (**Fig**

2). However, the shape of the bell was less well-defined in old than in young rats. The amplitude of the bell was higher in the young animals (*insets to Fig 2A and 2B*). At pretreatment, the shape and amplitude of hole exploration frequency was comparable in both senile groups ( $P=0.1$ ), and the hole 0 exploration frequency was significantly different than the rest of the holes in both senile groups (**Fig 2-A,  $P<0.0001$** ). After treatment, the shape and amplitude of hole exploration frequency was significantly different between Sc and Smsc groups ( $P=0.045$ ) with a major preference for holes neighboring goal hole than farther holes (**Fig 2-B,  $P<0.0001$** ). Notice that hole 0 exploration frequency of Smsc group was significantly higher than in Sc rats ( $P<0.01$ ). Also, there is a statistically significant interaction between treatment and hole position ( $P=0.008$ ).

**3.2.2- Goal sector exploration-** The hole exploration frequency of senile rats before and after MSC treatment was assessed and compared in different goal sectors. In GS1 Sc rats showed no significant difference before and after experimental day 0 ( $P=0.116$ ) whereas MSC treatment induced a significant increase in GS1 exploration (**Fig 3-B,  $P=0.016$** ). In the case of GS3, exploration frequency both old rat groups showed a significant difference before and after experimental day 0 ( $P=0.016$ ). In the Smsc rats, treatment induced a significant increase in GS3 exploration frequency (**Fig 3-C,  $P=0.015$** ). When as compared progression in the GS3 exploratory frequency (post-treatment - pre-treatment), Smsc rats presented an improvement in this parameter but Sc rats showed an impaired behavior (**Fig 3-D,  $P=0.001$** ).

### 3.3 Morphometric Changes

#### 3.3.1- Effects of MSCs treatment on hippocampal morphometry in old rats

A stereological assessment of neuroblasts and microglial cells was performed in the dorsal hippocampus of young and senile control rats as well as in MSCs-treated aged rats. There was a significant increase in the number of DCX cells (neuroblasts) in the DG of MSC-treated senile versus control senile rats. This could be seen at qualitative (**Fig 4-A, B, C**) and statistical level (**Fig 4**

**D, P=0.042**). As expected, the number of DCX neurons in the same region was much higher in young than in old rats (**Fig 4-D inset**). Hippocampal microglial cells were classified as non-reactive and reactive and were counted in the *Stratum Radiatum* (Srad). As expected, the number of reactive microglial cells increased with age but in the senile rats MSC treatment induced a significant decrease in the number of reactive Iba-1 immunoreactive cells as compared with senile control counterparts (**Fig 5-D, P=0.075**). Non-reactive microglial cell number in the MSC-treated senile rats was significantly increased as compared with senile controls (**Fig. 5-E, P=0.002**). MSC treatment induced no significant changes in total Iba-1 immunoreactive cells (**Fig 5-F, P=0.076**).

### 3.4 Synaptic protein changes after icv-MSCs administration

In order to explore the effect of MSCs in the senile hippocampus synapses, we determined the protein levels of three synaptic proteins by Western blot (WB) analysis (**Fig. 6-A**). SYP, a polypeptide component of small presynaptic transmitter-containing vesicles in neurons [30], neither age nor treatment induced changes in SYP levels (**Fig. 6-B, P=0.588**). However, SYT1, a synaptic vesicle-associated membrane protein that acts as calcium sensor for fast neurotransmitter release from presynaptic nerve terminals [31], showed significant decrease in senile rats (**Fig. 6-C, P=0.001**). Also, PSD-95, a membrane-associated guanylate kinase (MAGUK), that is the major scaffolding protein in the excitatory postsynaptic density and a potent regulator of synaptic strength [32], showed significant decrease in senile rats (**Fig. 6-D, P=0.0423**).

## 4.-DISCUSSION

Previous studies have shown that lifelong intravenous (iv) injection of amniotic membrane-derived hMSCs (AM-MSCs) or adipose tissue-derived MSCs (AD-MSCs) to 10-month-old male F344 had life-extending effects. The AM-MSCs and AD-MSC improved cognitive and physical functions of naturally aging rats, extending life span by 23 and 31%, respectively [33]. The above findings, as

well as results from others [34] and from our group suggest that MSCs possess the ability to slow down the age-related decline typical of higher animal species when the treatment is begun during adulthood. Thus, we have demonstrated that lifelong iv injection of hMSCs begun in a rat at 6 months of age, markedly prolonged (22%) lifespan (44 months versus the typical 36 months of standard laboratory rats [35, 36]). In the present study we focused our work on the effect of MSC treatment when begun in already old rats, in an attempt to determine whether administration of hBM-MSCs to aged rats could be able to restore their deficient cognitive performance and altered hippocampal morphology. Although the main goal of the study was to assess the possible restorative effects of MSC on spatial memory performance and hippocampal neurogenesis in old rats, the fact that an exploration of the restorative effects of mesenchymal cell therapy has, to our knowledge, never been reported in old rats prompted us to explore the effect of MSC-treatment in another relevant cell population, the microglia. Since old rats are highly valuable animals, we screened a number of structural and cellular features in the hippocampus of these rats and found that, besides spatial memory performance, microglial activity was also rescued by the treatment. Consequently, we deemed that reporting on the beneficial effect of the treatment on microglial reactivity was a valuable addition.

We chose the ependymal route of administration in order to avoid losing MSCs in extraneural compartments like liver and lungs. Since the time-course results reveal a slowly declining number of MSCs in the cerebroventricular space, it seems that the injected MSCs have a limited time-window of permanence in the cerebroventricular spaces of old animals. The rather modest number of Dil(+) cells in the brain parenchyma observed in our old rats differs from the findings reported in young rats icv injected with BM-MSCs [14]. The study reports that after transplantation, MSCs migrated mainly to the ipsilateral DG, CA1 and CA3 regions of the hippocampus, and to a lesser extent, to other regions of the brain. The authors used FSL rat-derived BM-MSCs whereas in our study human-derived BM-MSCs were used. This difference might account for the contrast between the migration

observed by Tfilin and co-workers in the brain of their rats and the limited migration of hMSC into the brain parenchyma of ours.

Concerning the effect of hBM-MSCs on behavior, our results showing an improvement induced by MSC-treatment in old rats on the accuracy to locate the goal sector in the Barnes maze are in line with documented evidence of cognitive improvement in mouse and rat models of neurodegenerative diseases. Thus, it has been reported that in an acute AD mouse model, intra-hippocampal administration of human umbilical cord blood-derived mesenchymal stem cells (hUC-MSCs) partially rescued cognitive performance as assessed by the Morris water maze test [37]. In a study mentioned above adult rat MSCs were injected ( $10^5$  cells/bilaterally) into the lateral ventricle of Flinders sensitive line (FSL), rats, an animal model for depression. When twelve days later, rats were assessed by the forced swim test and the dominant–submissive relationship paradigm, results revealed that MSCs-transplanted FSL rats had a significant improvement in their behavioral performance in both tests [14].

Our observation that MSCs-treatment significantly increased the number of DCX neurons in the DG of old rats suggests a mild but significant increase in either neurogenesis or mean half-life of neuroblasts in this region. Indeed, there is evidence that when implanted in the hippocampal DG of rodents, MSCs promote neurogenesis. Thus, it was reported that hMSCs implanted into the hippocampal DG of immunodeficient mice induced migration of BrdUrd-labeled endogenous cells throughout the dorsal hippocampus (positive for DCX). Some of the cells expressed markers for astrocytes and for neural or oligodendrocyte progenitors [9]. In the study by Tfilin *et al*, 2010, cited above, the authors reported that after icv transplantation, neurogenesis was increased in the ipsilateral hippocampal DG of engrafted rats (granular cell layer) and was correlated with MSCs engraftment and behavioral performance [14].

The initial assumption in exploring the mechanisms by which MSCs ameliorate central nervous system (CNS) injury was that they migrated to the injured tissues and transdifferentiated to replace

damaged neural cells [15, 16]. However, more recent studies showed that transplanted MSCs exert their therapeutic effect without evidence of engraftment [38–40], which indicates that their regenerative and differentiating abilities may not play a role in enhancing tissue repair or limiting tissue destruction.

Furthermore, it is known that when stimulated by inflammatory signals, MSCs secrete a variety of bioactive molecules, such as trophic factors and anti-inflammatory molecules able to modulate the host microenvironment [41], which is likely to be the main mechanism responsible for their therapeutic effects when they are administered iv or icv [42]. Some of the neurotrophic factors responsible for these effects are likely to come from the MSCs themselves as suggested by a study in which screening a human MSCs cDNA library revealed expressed transcripts encoding BDNF and  $\beta$ -NGF. Furthermore, immunostaining demonstrated that BDNF and  $\beta$ -NGF proteins were restricted to specific MSCs subpopulations, which was confirmed by ELISA analysis of 56 separate subclones of hMSCs [5]. Besides, neurotrophic factor-mediated protection was reported following human MSCs transplantation into rodent models of neurodegenerative diseases [see an extend revision in Volkman & Offen (2017), 43]. Therefore, the possibility exists that neurotrophic factors released by our hBM-MSCs into the cerebroventricular space reached hippocampal cells thus inducing a moderate improvement in function and structure.

Immune reactivity and inflammatory processes increase with aging in the brain [18], with microglia playing a central role in this immune dysregulation [19, 20]. Innate immunity within the central nervous system is primarily provided by resident microglia, brain cells that are essential in immune surveillance and that also mediate the coordinated responses between the immune system and the brain. With normal aging, microglia develop a more reactive phenotype. There are also major differences in microglial biology between young and old age when the immune system is challenged, and microglia activated. In this context, microglial activation is amplified and prolonged in the aged brain compared to adult brains. Prolonged microglial activation leads to the release of pro-

inflammatory cytokines that exacerbate neuroinflammation, contributing to neuronal loss and impairment of cognitive function [19, 20].

As expected, the number of reactive microglial cells in the Srad of our senile rats was significantly higher than in young controls but after hBM-MSc treatment the number of reactive microglial cells in the Srad of senile rats was back to young levels. This is in line with evidence that BM-MSCs maintain the resting phenotype of microglia and inhibit microglial activation through their production of several factors [20]. Neither aging nor MSC treatment appeared to modify the total number microglial cells in the Srad of our rats.

There is growing evidence in support of a relevant role of microglia in synaptic circuit remodeling [44–48]. Particularly, it was observed that microglia modulates synapses through elimination of presynaptic material [42, 45]. Additionally, a distinctive feature of aging is the cognitive deficit, which in the hippocampus correlates with altered synaptic morphology including loss of pre- and post-synaptic proteins [49]. The present study revealed a differential expression of synaptic protein in the hippocampus of senile rats; specifically, the presynaptic SYT1 and the postsynaptic PSD95 proteins are decreased. Interestingly, a single MSCs transplantation in these animals restored the SYT1 levels to young animal values. This observation is in line with a study in a conventional aging model in mice in which hUC-MSCs remarkably enhanced the synaptic plasticity in the CA1 area of aged hippocampus [50].

### **Conclusions**

We conclude that the restorative action of hBM-MSCs is stronger when they are used in adult animals as suggested by the life extension studies described above. The present results suggest that when very old rats are treated with hBM-MSCs the restorative effect is milder. Thus, it seems plausible to hypothesize that MSCs exert a stabilizing action on brain homeostasis rather than a restorative or rejuvenating effect. We used bone marrow MSCs from an adult donor; if bone marrow

MSCs from younger donors or umbilical cord-derived MSCs had been used in old rats, the effects might have been stronger.

### Conflicts of interest

There are no conflicts of interest concerning any of the authors.

### FUNDING

This work was supported by grants #PICT15-0817 from the Argentine Agency for the Promotion of Science and Technology and research grant MRCF 10-10-17 from the Medical Research Charitable Foundation and the Society for Experimental Gerontological Research, New Zealand to RGG and grant PICT 2015-1998 to PCR.

### ACKNOWLEDGEMENTS

The authors thank Ms. Natalia Scelsio, Ms. Romina Becerra and Ms. Juliette López Hanotte for technical assistance. Ms. Araceli Bigres for animal care assistance, and Ms. Yolanda E. Sosa for editorial assistance. MGG, GM, GRM, PCR, and RGG are career researchers of CONICET. MFZV and ML are recipients of CONICET doctoral fellowships. GMC is a researcher from CIC-PBA.

### REFERENCES

- [1] S. A. Hardy, D. J. Maltman, and S. A. Przyborski, "Mesenchymal stem cells as mediators of neural differentiation," *Curr Stem Cell Res Ther*, vol. 3, no. 1, pp. 43–52, Jan. 2008.
- [2] S.-H. Koh, M. Y. Noh, G. W. Cho, K. S. Kim, and S. H. Kim, "Erythropoietin increases the motility of human bone marrow-multipotent stromal cells (hBM-MSCs) and enhances the production of neurotrophic factors from hBM-MSCs," *Stem Cells Dev.*, vol. 18, no. 3, pp. 411–421, Apr. 2009.
- [3] D. J. Prockop, "Marrow stromal cells as stem cells for continual renewal of nonhematopoietic tissues and as potential vectors for gene therapy," *J. Cell. Biochem. Suppl.*, vol. 30–31, pp. 284–285, 1998.
- [4] J. E. Grove, E. Bruscia, and D. S. Krause, "Plasticity of bone marrow-derived stem cells," *Stem Cells*, vol. 22, no. 4, pp. 487–500, 2004.

- [5] L. Crigler, R. C. Robey, A. Asawachaicharn, D. Gaupp, and D. G. Phinney, "Human mesenchymal stem cell subpopulations express a variety of neuro-regulatory molecules and promote neuronal cell survival and neuritogenesis," *Exp. Neurol.*, vol. 198, no. 1, pp. 54–64, Mar. 2006.
- [6] H. Zhang, Z. Huang, Y. Xu, and S. Zhang, "Differentiation and neurological benefit of the mesenchymal stem cells transplanted into the rat brain following intracerebral hemorrhage," *Neurol. Res.*, vol. 28, no. 1, pp. 104–112, Jan. 2006.
- [7] J. Budni, T. Bellettini-Santos, F. Mina, M. L. Garcez, A. I. Zugno. "The involvement of BDNF, NGF and GDNF in aging and Alzheimer's disease," *Aging Dis.*, vol. 6, no. 5, pp. 331–341. Oct. 2015.
- [8] N. M. Ashpole, J. E. Sanders, E. L. Hodges, H. Yan, W. E. Sonntag, "Growth hormone, insulin-like growth factor-1 and the aging brain," *Exp Gerontol.*, vol. 68, pp. 76-81, Aug 2015.
- [9] J. R. Munoz, B. R. Stoutenger, A. P. Robinson, J. L. Spees, and D. J. Prockop, "Human stem/progenitor cells from bone marrow promote neurogenesis of endogenous neural stem cells in the hippocampus of mice," *Proc. Natl. Acad. Sci. U.S.A.*, vol. 102, no. 50, pp. 18171–18176, Dec. 2005.
- [10] S.W. Yoo, S.S. Kim, S.Y. Lee, H.S. Lee, H.S. Kim, Y.D. Lee, H. Suh-Kim, "Mesenchymal stem cells promote proliferation of endogenous neural stem cells and survival of newborn cells in a rat stroke model," *Exp. Mol. Med.*, vol. 40, no. 4, pp. 387–397, Aug. 2008.
- [11] M. Dezawa, "Systematic neuronal and muscle induction systems in bone marrow stromal cells: the potential for tissue reconstruction in neurodegenerative and muscle degenerative diseases," *Med Mol Morphol*, vol. 41, no. 1, pp. 14–19, Mar. 2008.
- [12] H. Hamada, M. Kobune, K. Nakamura, Y. Kawano, K. Kato, O. Honmou, K. Houkin, T. Matsunaga, Y. Niitsu, "Mesenchymal stem cells (MSC) as therapeutic cytoagents for gene therapy" *Cancer Sci.*, vol. 96, no. 3, pp. 149–156, Mar. 2005.
- [13] D. Karussis, I. Kassis, B. G. S. Kurkalli, and S. Slavin, "Immunomodulation and neuroprotection with mesenchymal bone marrow stem cells (MSCs): a proposed treatment for multiple sclerosis and other neuroimmunological/neurodegenerative diseases," *J. Neurol. Sci.*, vol. 265, no. 1–2, pp. 131–135, Feb. 2008.
- [14] M. Tfilin, E. Sudai, A. Merenlender, I. Gispan, G. Yadid, and G. Turgeman, "Mesenchymal stem cells increase hippocampal neurogenesis and counteract depressive-like behavior," *Mol. Psychiatry*, vol. 15, no. 12, pp. 1164–1175, Dec. 2010.
- [15] G. C. Kopen, D. J. Prockop, and D. G. Phinney, "Marrow stromal cells migrate throughout forebrain and cerebellum, and they differentiate into astrocytes after injection into neonatal mouse brains," *Proc. Natl. Acad. Sci. U.S.A.*, vol. 96, no. 19, pp. 10711–10716, Sep. 1999.
- [16] C. Qu, A. Mahmood, D. Lu, A. Goussev, Y. Xiong, and M. Chopp, "Treatment of traumatic brain injury in mice with marrow stromal cells," *Brain Res.*, vol. 1208, pp. 234–239, May 2008.
- [17] G. L. Barrett, A. Bennie, J. Trieu, S. Ping, and C. Tsafoulis, "The chronology of age-related spatial learning impairment in two rat strains, as tested by the Barnes maze," *Behav. Neurosci.*, vol. 123, no. 3, pp. 533–538, Jun. 2009.
- [18] K. M. Lucin and T. Wyss-Coray, "Immune activation in brain aging and neurodegeneration: too much or too little?," *Neuron*, vol. 64, no. 1, pp. 110–122, Oct. 2009.
- [19] X.-G. Luo, J.-Q. Ding, and S.-D. Chen, "Microglia in the aging brain: relevance to neurodegeneration," *Mol Neurodegener*, vol. 5, p. 12, Mar. 2010.
- [20] D. M. Norden and J. P. Godbout, "Review: microglia of the aged brain: primed to be activated and resistant to regulation," *Neuropathol. Appl. Neurobiol.*, vol. 39, no. 1, pp. 19–34, Feb. 2013.
- [21] J. Pardo, M.C. Abba, E. Lacunza, L. Francelle, G.R. Morel, T.F. Outeiro, R.G. Goya, "Identification of a conserved gene signature associated with an exacerbated inflammatory

- environment in the hippocampus of aging rats,” *Hippocampus*, vol. 27, no. 4, pp. 435–449, 2017.
- [22] K. Yan, R. Zhang, C. Sun, L. Chen, P. Li, Y. Liu, L. Peng, H. Sun, K. Qin, F. Chen, W. Huang, Y. Chen, B. Lv, M. Du, Y. Zou, Y. Cai, L. Qin, Y. Tang, X. Jiang, “Bone marrow-derived mesenchymal stem cells maintain the resting phenotype of microglia and inhibit microglial activation,” *PLoS ONE*, vol. 8, no. 12, p. e84116, 2013.
- [23] M. G. Garcia, J. Bayo, M.F Bolontrade, L. Sganga, M. Malvicini, L. Alaniz, J.B. Aquino, E. Fiore, M.M. Rizzo, A. Rodriguez, A. Lorenti, O. Andriani, O. Podhajcer, G. Mazzolini, “Hepatocellular carcinoma cells and their fibrotic microenvironment modulate bone marrow-derived mesenchymal stromal cell migration in vitro and in vivo,” *Mol. Pharm.*, vol. 8, no. 5, pp. 1538–1548, Oct. 2011.
- [24] G. Paxinos and C. Watson, “The rat brain in stereotaxic coordinates,” *Academic Press, San Diego*, 1998.
- [25] G. R. Morel, T. Andersen, J. Pardo, G.O. Zuccolilli, V.L. Cambiaggi, C.B. Hereñú, R.G. Goya, “Cognitive impairment and morphological changes in the dorsal hippocampus of very old female rats,” *Neuroscience*, vol. 303, pp. 189–199, Sep. 2015.
- [26] M. F. Zappa Villar, J. López Hanotte, E. Falomir Lockhart, L. S. Trípodí, G. R. Morel, and P. C. Reggiani, “Intracerebroventricular streptozotocin induces impaired Barnes maze spatial memory and reduces astrocyte branching in the CA1 and CA3 hippocampal regions,” *J Neural Transm (Vienna)*, Sep. 2018.
- [27] J. Glowinski and L. L. Iversen, “Regional studies of catecholamines in the rat brain. I. The disposition of [3H]norepinephrine, [3H]dopamine and [3H]dopa in various regions of the brain,” *J. Neurochem.*, vol. 13, no. 8, pp. 655–669, Aug. 1966.
- [28] M. J. West, “New stereological methods for counting neurons,” *Neurobiol. Aging*, vol. 14, no. 4, pp. 275–285, Aug. 1993.
- [29] Y. Diz-Chaves, O. Pernía, P. Carrero, and L. M. Garcia-Segura, “Prenatal stress causes alterations in the morphology of microglia and the inflammatory response of the hippocampus of adult female mice,” *J Neuroinflammation*, vol. 9, p. 71, Apr. 2012.
- [30] B. Wiedenmann and W. W. Franke, “Identification and localization of synaptophysin, an integral membrane glycoprotein of Mr 38,000 characteristic of presynaptic vesicles,” *Cell*, vol. 41, no. 3, pp. 1017–1028, Jul. 1985.
- [31] M.A. Fox and J.R. Sanes, “Synaptotagmin I and II are present in distinct subsets of central synapses,” *J Comp Neurol.*, vol. 503(2):280–96, Jul. 2007.
- [32] X. Chen, C. D. Nelson, X. Li, C. A. Winters, R. Azzam, A. A. Sousa, R. D. Leapman, H. Gainer, M. Sheng, and T. S. Reese, “PSD-95 is required to sustain the molecular organization of the postsynaptic density,” *J Neurosci*, vol. 31, no. 17, pp. 6329–6338, Oct. 2011.
- [33] D. Kim, J. Kyung, D. Park, E.K. Choi, K.S. Kim, K. Shin, H. Lee, I.S. Shin, S.K. Kang, J.C. Ra, Y.B. Kim, “Health Span-Extending Activity of Human Amniotic Membrane- and Adipose Tissue-Derived Stem Cells in F344 Rats,” *Stem Cells Transl Med*, vol. 4, no. 10, pp. 1144–1154, Oct. 2015.
- [34] J. Shen, Y.T. Tsai, N. M. Dimarco, M. A. Long, X. Sun, and L. Tang, “Transplantation of mesenchymal stem cells from young donors delays aging in mice,” *Sci Rep*, vol. 1, p. 67, 2011.
- [35] E. Mansilla, G. Roque, Y. E. Sosa, A. Tarditti, and R. G. Goya, “A Rat Treated with Mesenchymal Stem Cells Lives to 44 Months of Age,” *Rejuvenation Res*, vol. 19, no. 4, pp. 318–321, Aug. 2016.
- [36] R. A. Warmack, E. Mansilla, R. G. Goya, and S. G. Clarke, “Racemized and Isomerized Proteins in Aging Rat Teeth and Eye Lens,” *Rejuvenation Res*, vol. 19, no. 4, pp. 309–317, Aug. 2016.

- [37] H. J. Lee, J.K. Lee, H. Lee, J.W. Shin, J.E. Carter, T. Sakamoto, H.K. Jin, J.S. Bae, "The therapeutic potential of human umbilical cord blood-derived mesenchymal stem cells in Alzheimer's disease," *Neurosci. Lett.*, vol. 481, no. 1, pp. 30–35, Aug. 2010.
- [38] R. H. Lee, A.A. Pulin, M.J. Seo, D.J. Kota, J. Ylostalo, B.L. Larson, L. Semprun-Prieto, P. Delafontaine, D.J. Prockop, "Intravenous hMSCs improve myocardial infarction in mice because cells embolized in lung are activated to secrete the anti-inflammatory protein TSG-6," *Cell Stem Cell*, vol. 5, no. 1, pp. 54–63, Jul. 2009.
- [39] M. Janowski, D.C. Wagner, and J. Boltze, "Stem Cell-Based Tissue Replacement After Stroke: Factual Necessity or Notorious Fiction?," *Stroke*, vol. 46, no. 8, pp. 2354–2363, Aug. 2015.
- [40] N. Wang, Q. Li, L. Zhang, H. Lin, J. Hu, D. Li, S. Shi, S. Cui, J. Zhou, J. Ji, J. Wan, G. Cai, X. Chen, "Mesenchymal stem cells attenuate peritoneal injury through secretion of TSG-6," *PLoS ONE*, vol. 7, no. 8, p. e43768, 2012.
- [41] A. Scuteri, M. Miloso, D. Foudah, M. Orciani, G. Cavaletti, and G. Tredici, "Mesenchymal stem cells neuronal differentiation ability: a real perspective for nervous system repair?," *Curr Stem Cell Res Ther*, vol. 6, no. 2, pp. 82–92, Jun. 2011.
- [42] L. da S. Meirelles, A. M. Fontes, D. T. Covas, and A. I. Caplan, "Mechanisms involved in the therapeutic properties of mesenchymal stem cells," *Cytokine Growth Factor Rev.*, vol. 20, no. 5–6, pp. 419–427, Dec. 2009.
- [43] R. Volkman, D. Offen. "Concise Review: Mesenchymal Stem Cells in Neurodegenerative Diseases," *Stem Cells.*, vol. 35, no. 8, pp. 1867–1880. Aug. 2017.
- [44] L. Weinhard, G. di Bartolomei, G. Bolasco, P. Machado, N.L. Schieber, U. Neniskyte, M. Exiga, A. Vadisiute, A. Raggioli, A. Schertel, Y. Schwab, C.T. Gross, "Microglia remodel synapses by presynaptic trogocytosis and spine head filopodia induction," *Nat Commun*, vol. 9, no. 1, p. 1228, Mar. 2018.
- [45] R. C. Paolicelli, G. Bolasco, F. Pagani, L. Maggi, M. Scianni, P. Panzanelli, M. Giustetto, T.A. Ferreira, E. Guiducci, L. Dumas, D. Ragozzino, C.T. Gross, "Synaptic pruning by microglia is necessary for normal brain development," *Science*, vol. 333, no. 6048, pp. 1456–1458, Sep. 2011.
- [46] D. P. Schafer, E.K. Lehrman, A.G. Kautzman, R. Koyama, A.R. Mardinly, R. Yamasaki, R.M. Ransohoff, M.E. Greenberg, B.A. Barres, B. Stevens, "Microglia sculpt postnatal neural circuits in an activity and complement-dependent manner," *Neuron*, vol. 74, no. 4, pp. 691–705, May 2012.
- [47] G. O. Sipe, R. L. Lowery, M.-È. Tremblay, E. A. Kelly, C. E. Lamantia, and A. K. Majewska, "Microglial P2Y12 is necessary for synaptic plasticity in mouse visual cortex," *Nat Commun*, vol. 7, p. 10905, Mar. 2016.
- [48] M.È. Tremblay, R. L. Lowery, and A. K. Majewska, "Microglial interactions with synapses are modulated by visual experience," *PLoS Biol.*, vol. 8, no. 11, p. e1000527, Nov. 2010.
- [49] B. Ojo, P. Rezaie, P.L. Gabbott, H. Davies, F. Colyer, T.R. Cowley, M. Lynch, M.G. Stewart. "Age-related changes in the hippocampus (loss of synaptophysin and glial-synaptic interaction) are modified by systemic treatment with an NCAM-derived peptide, FGL," *Brain Behav Immun*, vol. 26, no. 5, pp. 778–88, Jul. 2012.
- [50] N. Cao, T. Liao, J. Liu, Z. Fan, Q. Zeng, J. Zhou, H. Pei, J. Xi, L. He, L. Chen, X. Nan, Y. Jia, W. Yue, and X. Pei, "Clinical-grade human umbilical cord-derived mesenchymal stem cells reverse cognitive aging via improving synaptic plasticity and endogenous neurogenesis," *Cell Death Dis*, vol. 8, no. 8, p. e2996, 10 2017.

**FIGURE LEGENDS**

**Figure 1. Experimental Design and time-course of hBM-MSCs after icv injection.** **Panel A-** illustrates the experimental design of the study. All animals were submitted to 2 daily acquisition trial from experimental day -9 to -6 and to a probe trial on experimental day -5. The hBM-MSCs were stereotaxically injected in the LV of Smsc rats on experimental day 0. Yc and Sc remained intact. From experimental day 15 to 18 all rats received a second (post treatment) series of acquisition trial and a probe trial on experimental day 18. On experimental day 21 rats were sacrificed, perfused with fixative and the brains removed for morphological analysis. **Panel B-** Fluorescence microscopy of ventricular brain sections at different times after labeled hBM-MSCs icv injection. After injection, hBM-MSCs numbers in the ventricular spaces declined slowly with most of the cells remaining in contact with the ependymal cell layer. A moderate number of Dil-labeled cells can be observed into the brain parenchyma near the ependymal cell layer. None was observed near the DG or other brain structures distant from the ventricular spaces. Abbreviation: Hab, *habituation*; LV, *lateral ventricle*; DG, *dentate gyrus*. Scale bar, 500  $\mu\text{m}$ .

**Figure 2. Effect of MSC therapy on hole exploration frequency.** At pretreatment (**Panel A**) both groups showed a similar exploratory frequency around hole #0. After treatment (**Panel B**) the exploration frequency of the MSC-treated senile rats for hole # 0 and 1, was significantly higher than those of the intact counterparts. Exploration frequency in the other holes remained similar for Sc versus Smsc rats for the equivalent holes in the platform. Insets show hole exploration frequency of Yc. Notice that hole exploratory frequency in young rats is 2.5-fold higher around the escape hole than in the senile counterparts. N=8 per group. All data is represented as mean  $\pm$  SEM. \*P<0.05 versus corresponding senile control.

**Figure 3. Effect of MSCs treatment on sector exploration frequency.** **A)** Diagrammatic representation of Barnes maze sectors (GS1 and GS3). **B)** GS1 exploratory frequency. The Sc group shows no significant pre- versus post-treatment changes, but Smsc rats significantly increased exploratory frequency. **C)** In the GS3 exploratory frequency Sc and Smsc show significant post-treatment changes namely, a decline for Sc and an increase for Smsc. **D)** The bar plot represents the progression in the GS3 exploratory frequency. It showed a positive progression in the Smsc rats and a negative progression in the Sc group. Abbreviations: GS, *goal sector*. N=8 per group. All data is represented as mean  $\pm$ SEM. \*P<0.05; \*\*\*, P<0.001.

**Figure 4. Doublecortin (DCX) expression in the dentate gyrus (DG) of young intact, senile intact and senile+MSCs rats. Images:** Coronal sections of the DG in representative animals of Yc (**A**), Sc (**B**), and Smsc (**C**) showing DCX neurons. **D** panel corresponds to a plot showing DCX cell numbers in the DG of senile rats. The inset shows DCX cell number in the same hippocampal region of Yc rats. Abbreviations: dh, *dentate hilus*; gcl, *granular cell layer*; ml, *molecular layer*. N=4 per group. All data is represented as mean  $\pm$ SEM. Comparisons were made between senile groups, \*P<0.05. Scale bar: 25  $\mu$ m.

**Figure 5. Iba-1 immunoreactive cells in the *Stratum Radiatum* of MSC-treated senile rats:** Coronal sections of the dorsal hippocampus in representative animals of each group showing Iba-1 immunoreactive cells. Left photomicrographs of Yc (**A**), Sc (**B**), and Smsc (**C**) groups show Iba-1 positive cells in the Srad. Right plots show the reactive (**D**), nonreactive (**E**) and the total number of microglia (**F**) in the Srad in the Yc, Sc, and Smsc rats. Abbreviations: Srad, *Stratum radiatum*, and py, *Stratum pyramidale*. N=4 per group. All data is represented as mean  $\pm$  SEM. Comparisons were made versus the Sc group, \*\*P<0.01; \*\*\*P<0.001. Scale bar: 50  $\mu$ m.

**Figure 6. MSCs therapy effect on rat hippocampal protein levels.** Images of VIN, SYT1, SYP, PSD95, and  $\beta$ -actin hippocampus protein levels of each animal (A). Quantification of protein levels of SYP (B), SYT1 (C), normalized to the relative density of VIN, and PSD95 (D) normalized to the relative density of  $\beta$ -actin. A significant decrease in SYT1 and PSD95 protein levels was observed in the Sc rats, while cell therapy led to a recovery of SYT1 level in the Smsc rats. SYP protein levels tend to decrease in the Sc group, but no significant differences are observed between both experimental groups. Abbreviation: *VIN*, Vinculin; *SYT1*, synaptotagmin 1; *SYP*, synaptophysin; *PSD95*, postsynaptic density protein 95. N=4 per group. All data is represented as mean  $\pm$ SEM. Comparisons were made between groups, \*P<0.05; \*\*\*P<0.001.

Fig 1

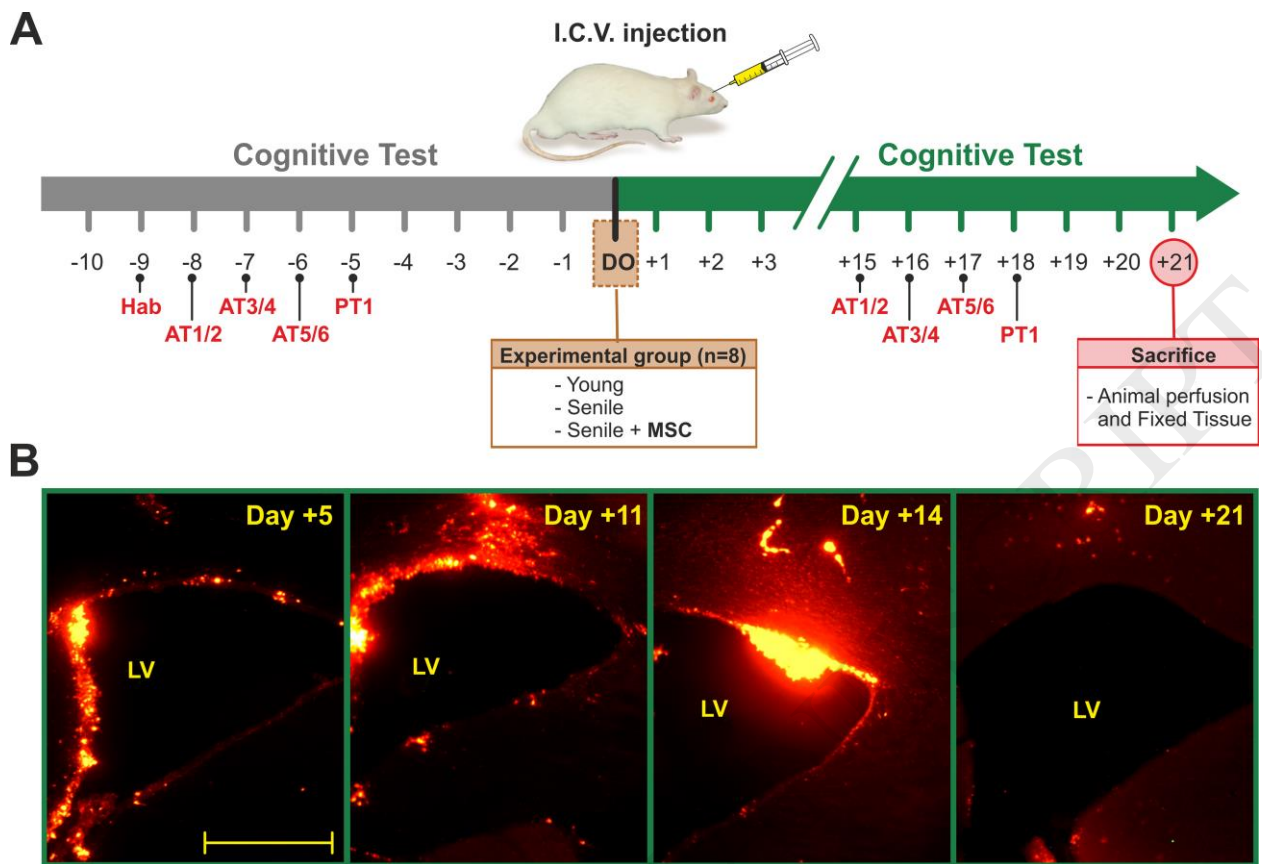


Fig 2

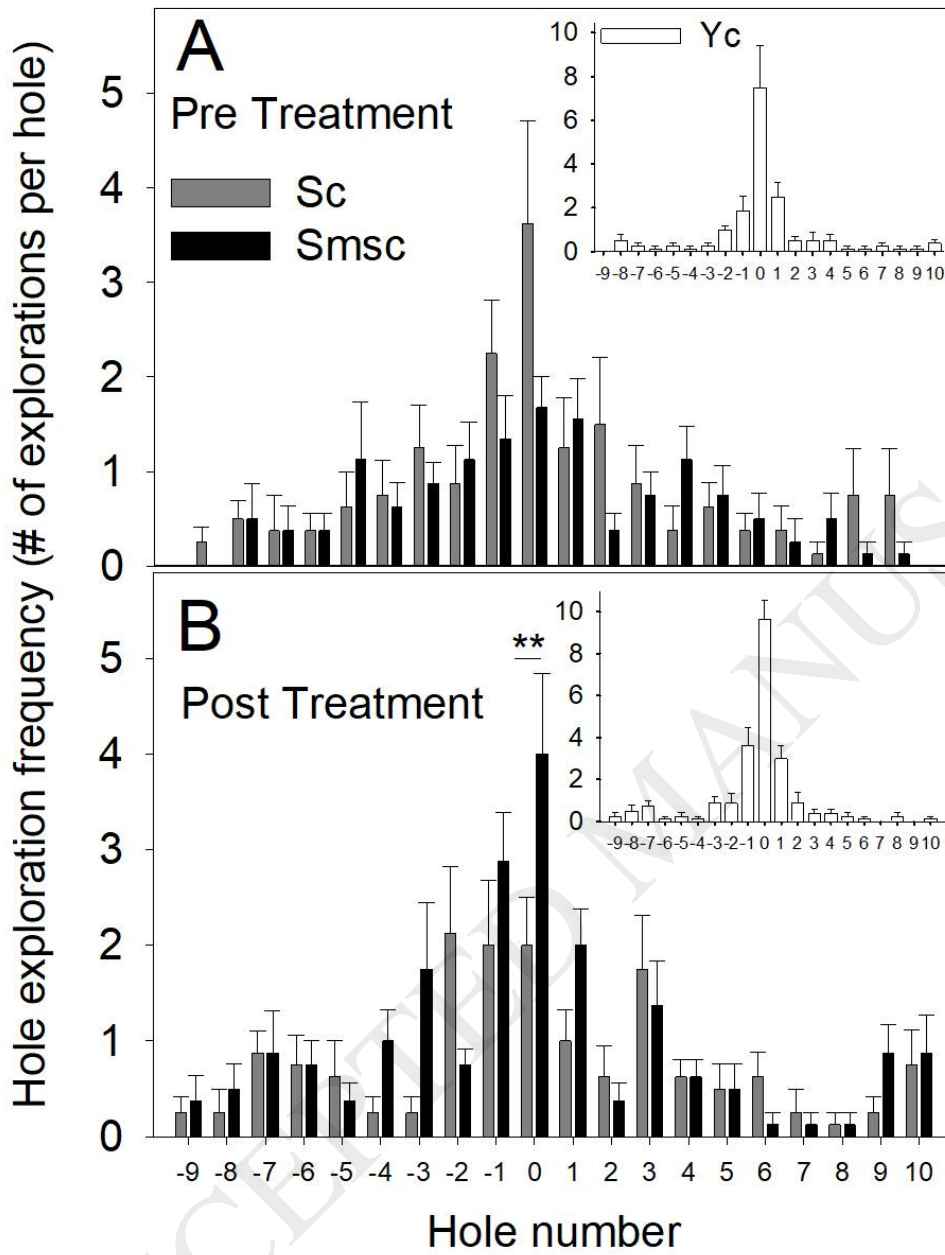


Figure 2

Fig 3

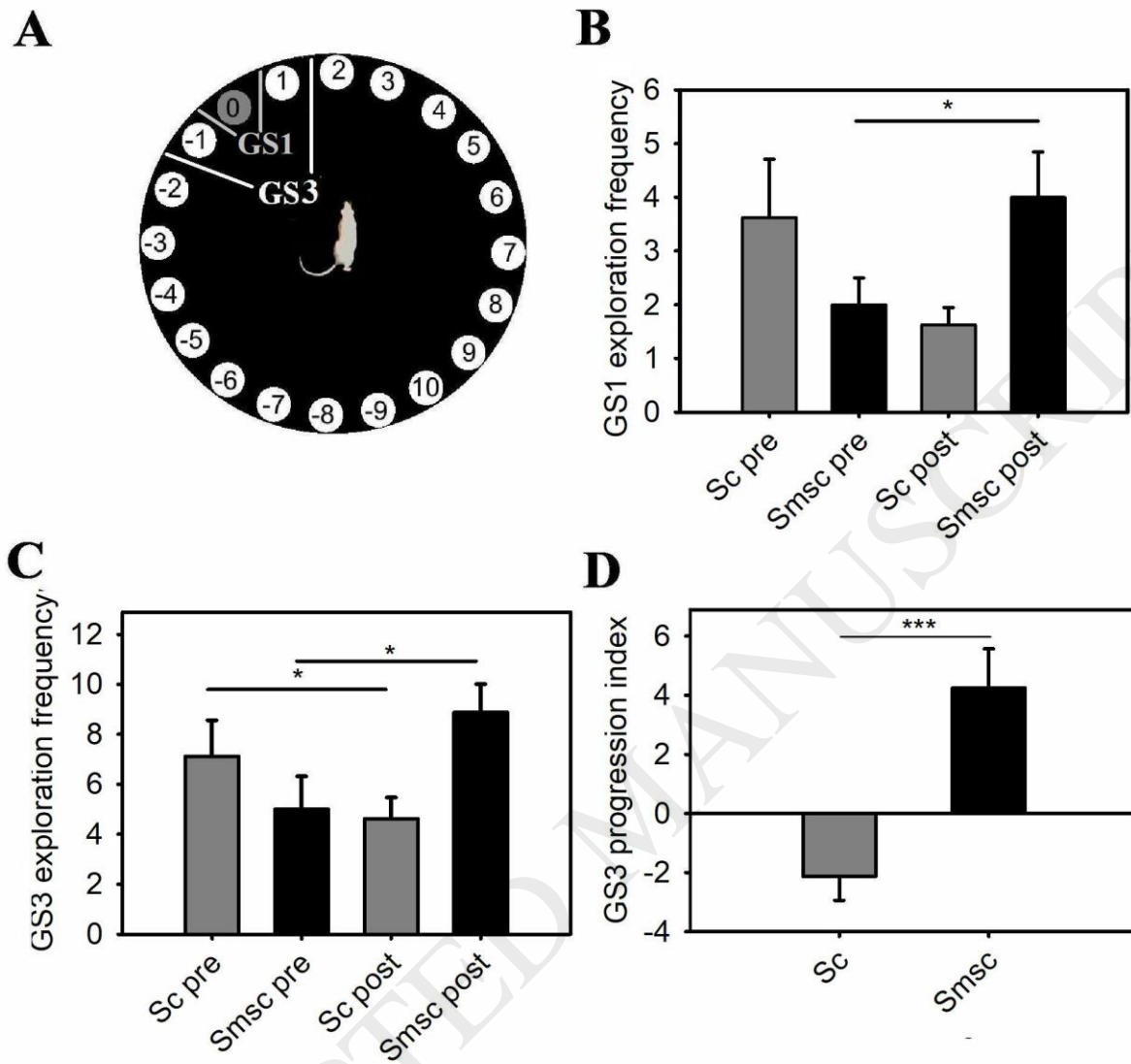


Figure 3

Fig 4

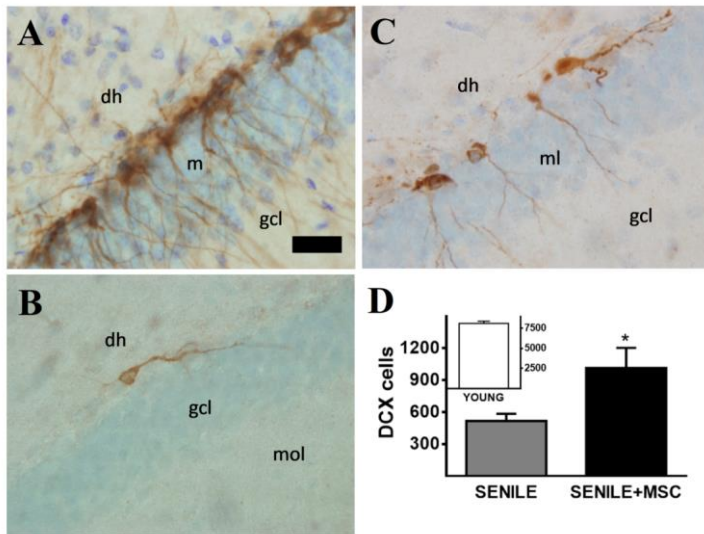


Fig 5

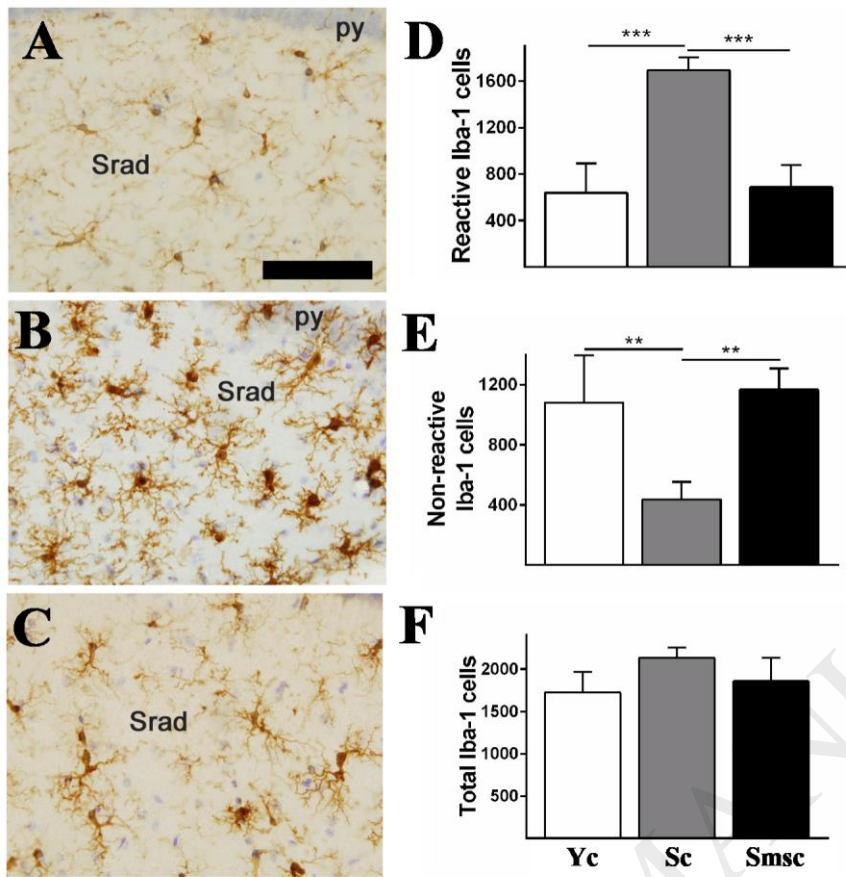


Fig 6

